# Photo-control of bimolecular reactions: reactivity of the long-lived Rhodamine 6G triplet excited state with ˙NO

Luke Macaleese, Bun Chan, Mathilde Bouakil, Philippe Dugourd, Richard O'hair

ARTICLE

# Photo-control of bimolecular reactions: reactivity of the long-lived Rhodamine 6G triplet excited state with ˙NO.

Received 00th January 20xx,
Accepted 00th January 20xx

DOI: 10.1039/x0xx00000x

Luke MacAleese,*[a] Bun Chan,[b] Mathilde Bouakil,[a] Philippe Dugourd[a] and Richard A. J. O'Hair*[c]

Photo-chemistry provides a non-intuitive but very powerful way to probe kinetically limited, sometimes thermodynamically non-favored reactions and, thus, access highly specific products. However, reactivity in the excited state is difficult to characterize directly, due to short lifetimes and challenges in controlling the reaction medium. Among photo-activatable reagents, rhodamine dyes find widespread uses due to a number of favorable properties including their high absorption coefficient. Their readily adaptable synthesis allows development of tailor-made dyes for specific applications. Remarkably, few studies have directly probed the chemical reactivity of their triplet excited state. Here we present a new conceptual approach to examine the specific chemistry of the triplet excited state. We have developed a pump (488nm) – probe (600nm) strategy to examine the gas-phase lifetime and reactivity of the triplet cation of Rhodamine 6G ($^3$Rh6G$^+$) in an ion trap mass spectrometer. The confounding effects of solvent, aggregation and formation of other reactive intermediates is thus avoided allowing fundamental reactivity to be explored. In the presence, in the ion trap, of helium seeded with 1 % of nitric oxide (˙NO) (~ 60 ion/˙NO collisions per second), the triplet lifetime is shortened from from 1.9 s to 0.7 s. Simultaneously, the reaction products [Rh6G -H]$^{\bullet+}$ and [Rh6G -H +NO]$^+$ are observed. Reaction of $^3$Rh6G$^+$ with ˙$NO_2$ yields [Rh6G -H]$^{\bullet+}$, [Rh6G -H +$NO_2$]$^+$ and [Rh6G -2H]$^+$. None of these products are observed for the singlet, $^1$Rh6G$^+$. DFT calculations suggest a stepwise mechanism only allowed from $^3$Rh6G$^+$, in which H atom abstraction by ˙$NO_x$ (x = 1 or 2) yields [Rh6G -H]$^{\bullet+}$ which, then, reacts with another ˙$NO_x$ molecule. This illustrates the power of light to initiate specific chemical reactions, and the relevance of gas-phase ion-molecule reaction approaches to understand stepwise reaction mechanism from specific excited states.

## Introduction

Rhodamine dyes find widespread uses as fluorescent probes due to a number of favorable properties including their high absorption coefficient, broad fluorescence in the visible region and high fluorescence quantum yield. Their readily adaptable synthesis[1] allows development of tailor-made dyes for specific applications, which include: environment-sensitive probes to study cellular processes;[2] reactive probes to act as "chemodosimeters" for biologically relevant metal ions, anions and thiols;[3,4] Förster resonant energy transfer (FRET) based probes for bioimaging;[5] photoredox catalysts in visible light mediated arylation reactions.[6] Remarkably, few studies have directly probed the chemical reactivity of the triplet excited state. Exceptions include the reactions of triplet Rhodamine 6G ($^3$Rh6G$^+$) with bases, which established that proton transfer could occur (Scheme 1A),[7] and with small molecules, which highlighted that only certain species such as oxygen, nitroxyl radicals and cyclooctatetraene quench the triplet state (Scheme 1B).[8]

As part of an ongoing series of gas-phase photofragmentation studies on rhodamine and related dyes aimed at developing "action FRET" as a probe for biomolecular structure,[9,10] we have been examining the fundamental photochemistry of Rhodamine based dyes.[11–13] We were, thus, intrigued by reports on long-lived gas-phase $^3$Rh6G$^+$ generated *via* photoexcitation of $^1$Rh6G$^+$ at 488 nm.[14,15] Reported lifetimes of seconds in an ion trap mass spectrometer are orders of magnitude longer than in solution,[16] in contrast with fluorescence lifetimes which scarcely vary and remain in the ns range.[17,18] These extra-ordinary long lifetimes enable the exploration of the specific chemical reactivity of rhodamine triplets via bimolecular ion-molecule reactions with neutral reagents. It also points out the potential of gas-phase approaches to explore photo-chemistry in general.

There is a rich history of studying the gas-phase ion-molecule reactions of atomic and small molecular cations that are electronically and/or vibrationally excited and state selected (see for lead references[19–31]). However, here, we take advantage of this long gas-phase life-time to provide one of the first examples where the chemistry of singlet and triplet forms

[a] *Univ Lyon, Université Claude Bernard Lyon 1, CNRS - Institut Lumière Matière (iLM), F-69622, LYON, France.*
[b] *Division of Chemistry and Materials Science, Nagasaki University - 1-14 Bunkyo, Nagasaki, 852-8521, Japan.*
[c] *School of Chemistry, University of Melbourne - Parkville, Victoria 3010. Australia.*

Electronic Supplementary Information (ESI) available: Full experimental and theoretical methods. Parameters for the collision rate calculation. Details of the rate constant extraction. CID efficiency as a function of NCE value. CID MS on singlet vs. triplet. Effect of isolation width on triplet deactivation. Product abundance as a function of collisional vs. laser activation. Simultaneous fits on fragments and products per dataset. Cartesian coordinates, charge and spin state of systems used for the computational approach. See DOI: 10.1039/x0xx00000x

of a large organic cation are directly compared in the absence of confounding effects of solvent, aggregation and formation of other reactive intermediates. Reactivity in the excited state, typically charge transfers, may be ultrafast. However, triplets live longer and are, thus, more prone to react with other molecules: triplet mediated delayed reactivity enables reagent diffusion and is often thought to be involved in catalytic cycles. Reaction means alteration of the original properties of the species, which may be something to avoid (*e.g.* bleaching for chromophores) but also production of new species difficult to attain by conventional (ground state) chemistry.

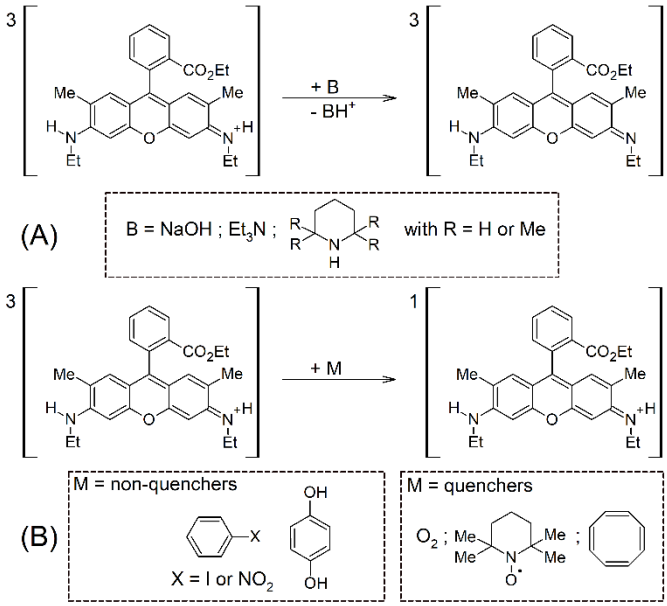


Scheme 1. Previous studies on the reactions of triplet Rhodamine 6G: (A) proton transfer reactions;[7] (B) molecules that can and cannot quench the triplet.[8]

The whole fields of photo-chemistry and photo-catalysis are paved with photo-induced spin changes and hypotheses of specific reactivity of triplet states. Metal-based photo-catalysis is often thought to involve low to high spin transitions and associated metal-ligand-charge-transfer states weakening bonds and enabling chemical reactions between ligands. The linkage isomerization of dimethylsulfoxide (DMSO) on a Ruthenium center that was described theoretically[32] and also reported experimentally in our group[33,34] is typically such a photo-induced mechanism involving multiple absorption events from low-spin singlets followed by singlet-to-triplet transitions where isomerization reactions can take place. Triplets may be considered as the bi-radical counterpart[35,36] of photo-induced free-radicals which have been proposed (or, more precisely, "intuited", see Thomas Tidwell's historical account[37]) as early as 1879 by Downes and Blunt.[38] Whereas the chemical integrity and atomic connectivity of triplets are maintained compared to their ground state singlet counterpart, photo-induced free radicals result from the dissociation of the irradiated precursor molecule. Both, nevertheless, possess unpaired electrons which are the foundation of their specific reactivity. It is, thus, expected that triplets chemistry is as rich and important as the well described free radical specific reactivity. This paper presents our efforts to produce and test the reactivity of Rhodamine 6G triplet cations in the gas phase.

## Experimental

See ESI for full details on materials and experimental methods as well as for theoretical approaches. Briefly, experiments were performed in a linear quadrupole ion trap mass spectrometer (LTQ Velos, Thermo Fisher Scientific, San Jose, CA), previously modified to allow interaction with lasers.[39] The $^{1}Rh6G^{+}$ cation was generated by electrospray ionization of a $10^{-5}$ M solution of Rh6G chloride salt (Lamba Physics GMBH) in methanol. A 488 nm continuous wave (CW) diode laser (COBOLT MLD 0488-06-01-200-100), was used to generate $^{3}Rh6G^{+}$. A Horizon OPO (Continuum, Santa Clara, CA) was used to record visible photo-dissociation spectra, and in particular was set at 600 nm to probe the triplet population by LID. For ion-molecule reactions, helium seeded with 1 % $^{\bullet}$NO (Air Liquide, Bagneux, France) was injected in the ion trap. Standard computational chemistry calculations were carried out with Gaussian 16.[40]

## Results and Discussion

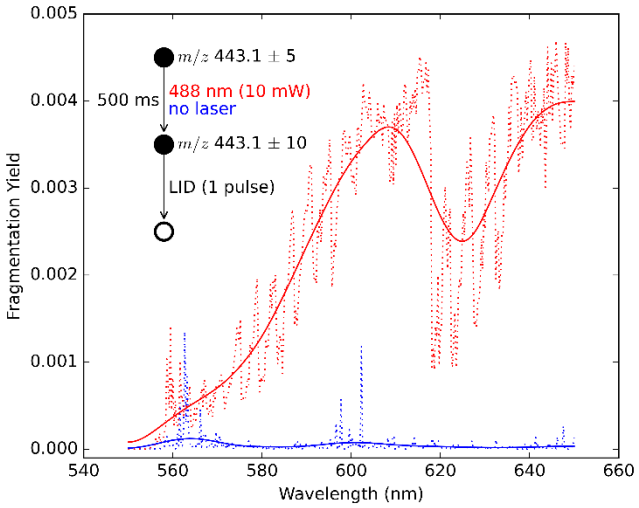


Figure 1. Photodissociation action spectrum of the Rhodamine 6G cations on the 550-650 nm range after 500 ms irradiation at 488 nm (red line) or 500 ms without irradiation (blue line). Raw data (dotted lines) were smoothed (solid lines). Ordinates are not normalized. Acquisitions were performed successively, one immediately after the other, under identical conditions and during the same experimental session. The difference thus reflects the differential absorption due to the triplet population.

### Triplet formation, spectroscopy and fragmentation

The very high fluorescence quantum yield (0.95) reported for Rh6G in solution[41] (likely to be increased in the desolvated ions[42]) implies that the inter-system crossing to the triplet state has only a very minor chance to occur per absorption event. However, once populated, triplets may live longer than excited singlets and up to seconds in the gas phase. Therefore the strategy used by Schooss *et al.* was employed here. It consists of cycling over the S1 ← S0 transition during seconds with a continuous wave (CW) laser in order to slowly build up the

triplet population at the expense of the ground state singlet. Unlike the experiments of Schooss *et al.*, where evidence for $^3Rh6G^+$ is established by detection of the successive loss and recovery of the singlet fluorescence emission,[14,15] the first major challenge was to develop an "action spectroscopy" method to specifically identify and differentiate the (isobaric) $^1Rh6G^+$ and $^3Rh6G^+$ formed upon photoexcitation. The optical photofragmentation spectra of $^1Rh6G^+$ (488 nm laser OFF) and $^3Rh6G^+$ (488 nm laser ON) are compared in Figure 1 and show that, at around 600 nm, only $^3Rh6G^+$ absorbs. This photo-fragmentation spectrum is similar to the transient absorption spectra observed in solution, where a maximum is also found around 600 nm.[43,44]

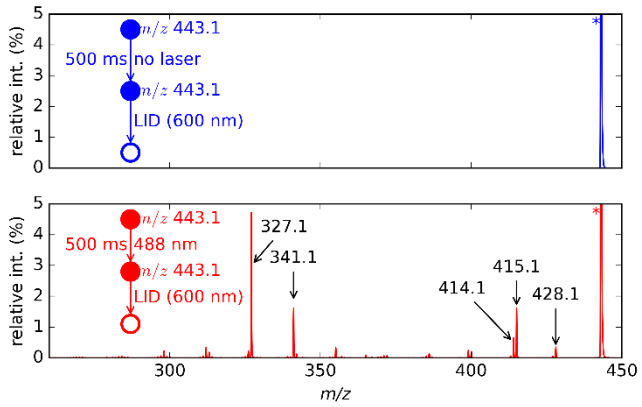


Figure 2. Comparison between LID spectra at 600 nm (1 single pulse, 8 mJ) of $Rh6G^+$ cation after 500 ms **without** (top: singlet only) and **with** (bottom: triplet is formed) irradiation at 488 nm (10 mW, 500 ms). Intensities are relative to the precursor (indicated with a "*").

Importantly, the specific laser induced dissociation (LID) of $^3Rh6G^+$ at 600 nm provides diagnostic photo-fragment ions at *m/z* 415.1, 341.1, 327.1, and 428.1, 414.1 which are not formed for $^1Rh6G^+$ (Figure 2). While the $C_2H_4$ loss ($\Delta m/z$ = 28) yielding the ion at *m/z* 415.1 represents the exclusive fragmentation path observed by collision-induced dissociation (CID) in our experimental conditions (see Figure S2), Ferreira *et al.* reported fragment ions at *m/z* 341.1 and 327.1 were derived from subsequent fragmentation of the initially formed ion at *m/z* 415.1 *via* radical-driven mechanisms.[45] Finally, the last two fragments, at *m/z* 428.1 and 414.1, are respectively assigned to losses of Me$^\bullet$ and Et$^\bullet$ originating from radical-driven cleavages (Scheme S1).

The presence of the latter direct radical-driven fragments which are not observed by CID (and have been discounted for the CID of singlet Rhodamine B[46]), as well as the predominance (on the contrary to CID spectra[45]) of secondary radical-driven fragments, thus, attest to the radical nature of the triplet electronic state from which rhodamine dissociates at 600 nm. Our DFT calculations suggest that the losses of both Me$^\bullet$ and Et$^\bullet$ are likely to occur from an N-ethyl group, with the former process yielding an $-N^+HCH_2$ moiety that is presumably stabilized through conjugation with the aromatic system (Scheme S1). The reaction energies for the production of Me$^\bullet$ and Et$^\bullet$ are respectively 148 and 164 kJ.mol$^{-1}$ for $^3Rh6G^+$, but they are much higher for $^1Rh6G^+$ (> 300 kJ.mol$^{-1}$).

The specific photo-fragmentation of $^3Rh6G^+$ is thus demonstrated. It incidentally confirms the actual formation of a significant triplet population after irradiation at 488 nm. However, since CID is widely used to characterize the unimolecular chemistry of ionic species, we nevertheless compared the CID spectra of $^1Rh6G^+$ and $^3Rh6G^+$ with Helium. Their CID characteristics, both in terms of fragmentation pattern and fragmentation threshold, are essentially the same (Figures S1 and S2): the unique fragment ion, in both case at *m/z* 415.1, arises, as mentioned earlier, from the loss of $C_2H_4$ and appears around 25 % normalized collision energy (NCE).[§,47] This suggests that collisional activation leads to quenching of the triplets (which were formed, as ascertained by the 600 nm probe) before ion fragmentation.

The effect of collisional heating on the triplet quenching was further investigated with the following pump-probe approach: monitoring the LID as a function of the NCE value. The decay curve observed in Figure S3 (right panel) can be fitted with a mono-exponential model that indicates that the NCE value associated with triplet quenching is very low: approximately 0.5 % NCE, *i.e.* much smaller than the fragmentation threshold. Moreover, the isolation window width is also shown to have a very strong effect on the LID yield (Figure S3, left panel). This is consistent with prior reports showing that collisional excitation with narrow isolation may fragment weakly bound non covalent complexes[48] and induce low-energy structural rearrangement reactions.[49] Both the CID behavior of $^3Rh6G^+$ and its quenching at narrow isolation windows confirm the extreme sensitivity of the triplet lifetime to collisional heating.

In summary, while CID activation proved to deactivate the triplets, irradiation around 600 nm was shown to induce their specific photo-fragmentation. This specificity was confirmed by the nature of the photo-fragments observed. Thus, the optical pump-probe strategy described above was adopted in order to monitor the evolution of the triplet state population, whereby irradiation of trapped, ground state $^1Rh6G^+$ with a CW laser at 488 nm was followed, after varying delays, by irradiation using a tunable laser (optical parametric oscillator, OPO) set at 600 nm.

### Evolution of the triplet population: lifetime and quenching under various gas conditions

The evolution of the triplet population was first evaluated under standard trapping gas conditions (Helium), following the optical pump-probe strategy described above: monitoring the photo-fragmentation ratio at 600 nm as a function of the relaxation time after 488 nm irradiation (Figure 3, Helium series). Multiple repeats were recorded, and the resulting fragmentation ratios systematically display mono-exponential decays. Least-square fitting is performed with the decay constant as common variable to all datasets acquired under standard ion trap conditions (pure helium buffer gas and room temperature). This yields an effective triplet lifetime in helium of 1878 ± 23 ms (2σ), which is in good agreement with the literature (2060 ms).[15] Given the very inefficient quenching of the triplet by collisions

with rare gas atoms,[14] the measured lifetime is probably radiation limited and the helium pressure difference (< 0.4 $10^{-3}$ mbar here *vs.* 0.2 mbar reported in ref [15]) should not come into play. The small lifetime difference may essentially arise from potential traces of the efficient triplet quencher $O_2$ in the trapping gas or from the different temperatures of the ion traps (≥ 298 K here *vs.* 286 K in ref[15]) acting on radiative and non-radiative processes.

Secondly, the triplet lifetime was checked in the presence of •NO (seeded at 1 % in the helium buffer gas) in the trap (Figure 3, •NO series). The capture rate constant between the ion and polar •NO, calculated *via* the Colrate program[50] using the Average Dipole Orientation (ADO) theory which is well adapted to describe ion-polar molecule collisions,[51] was found to be 5.8 $10^{-10}$ $cm^3.s^{-1}$. The number density of neutral •NO was calculated on the basis of the specified pressure (3.5 $10^{-4}$ Torr [52]) in the low pressure ion trap (LPT) where ion-molecule reactions are performed: ~ $10^{11}cm^{-3}$. However, the ion trap was modified and, in particular, the diameter of the aperture in the electrode separating the LPT from the vacuum manifold was significantly enlarged (up to 5 mm, *i.e.* factor 3-5 with respect to the original dimension). Thus, the leak rate must be significantly higher and the actual ion trap pressure lower than specified. In the worst case, the pressure in the trap is identical to that in the vacuum manifold, measured around $10^{-5}$ Torr, *i.e.* 1 order of magnitude smaller than specifications. Under the latter boundary conditions, the number density of •NO is, thus, similarly, ~ 1 order of magnitude smaller (~ $10^{10}$ molec.$cm^{-3}$). As a result, the actual collision rate between $^3$Rh6G$^+$ and •NO, calculated by multiplying the capture rate constant by the number density, is bound between ~ 6 and ~ 60 ion/•NO collisions per second.

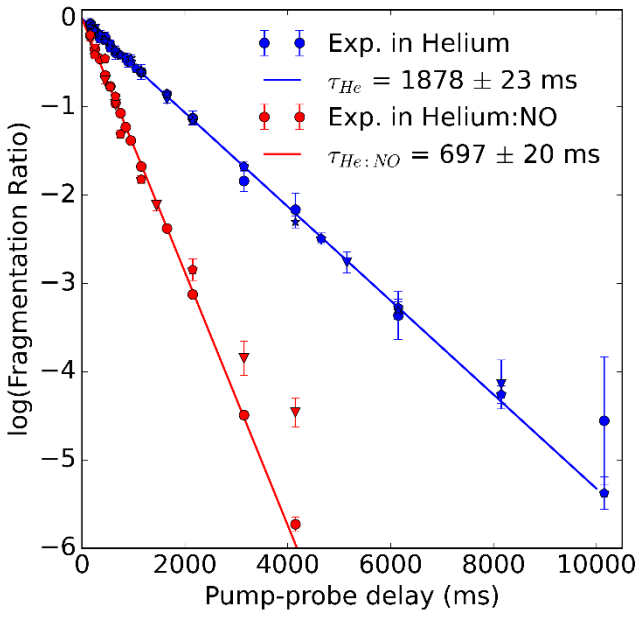


Figure 3. Evolution of the log of the fragmentation ratio of Rh6G$^+$ at 600 nm as a function of the delay between the end of the 500 ms irradiation at 488 nm and the 600 nm probe. Multiple experimental datasets are represented with different markers, in Helium (blue, 4 sets) and Helium:NO (1%) (red, 3 sets). All datasets were fitted simultaneously for each buffer gas conditions with a simple mono-exponential decay function and the decay constants as common parameters ($k_q^{He}$and $k_q = k_q^{He} + k_q^{NO}$). Then they were plotted together after substraction of their individual offset values and division by their individual pre-exponential factor. Time constants are indicated with 2$\sigma$ uncertainty windows.

Interestingly, despite this very low collision rate, the triplet lifetime falls to 697 ± 20 ms in the presence of •NO. While it remains very long compared to solution phase values, this corresponds to a nearly 3-fold decrease of the triplet lifetime with regards to pure helium conditions. Collisions with the molecular oxygen triplet is known to quench triplets very efficiently: in particular it was reported by Schooss *et al.* that, with only 1% $O_2$ in the ion trap (amounting in their pressure conditions to ~2 $10^4$ ion/$O_2$ collisions per second), the $^3$Rh6G$^+$ lifetime was too short to be measured.[14,15] Collisions with radical •NO is similarly expected to quench the rhodamine triplet.

In any case, the additional triplet decay mechanisms associated with •NO are independent from the radiative decay measured in helium. Thus, the new rate constant determined in the presence of •NO (~1.4 $s^{-1}$) corresponds to the sum of the radiative decay constant determined in pure He (~0.5 $s^{-1}$) and of the •NO-associated triplet decay rate. As a consequence, one can estimate the latter between 0.8 - 0.9 $s^{-1}$. Given the estimated collision rate range, the triplet decay probability *per* collision can then be estimated between 1 and ~ 13-15 %. While these probabilities are high, they are considerably lower than reported quenching by $O_2$. As a reminder, the triplet deactivation probability was estimated above 50 % in the case of $O_2$.[14]

### Triplet reactivity: case of •NO (and •$NO_2$)

Preferential quenching with •NO *vs.* helium is most likely due to the enhanced electronic interaction between triplet $^3$Rh6G$^+$ and doublet •NO. Additionally, when electronic interaction is optimal, the chemical reactivity may modify the systems and yield reaction products, which may also contribute to the significant shortening of the lifetime of $^3$Rh6G$^+$. The reactivity of the triplet with •NO was examined as illustrated in Figure 4.

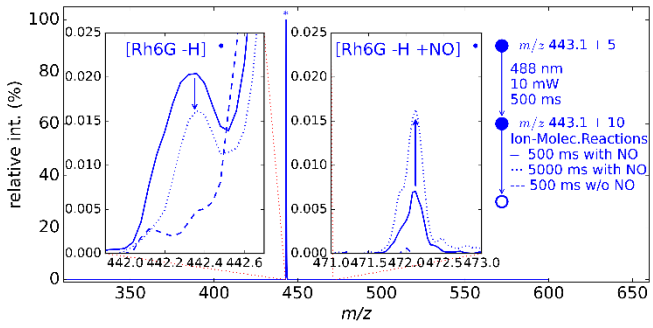


Figure 4. Mass spectra measured after 500 ms irradiation at 488 nm (MS$^2$) followed by an MS$^3$ step of either 500 ms in presence of •NO (—), or 5000 ms with •NO (••••), or 500 ms without •NO (---). Left and right inserts focus on the $[Rh6G - H]^{\bullet+}$ and $[Rh6G - H + NO]^+$ product ion peaks, respectively. Intensities expressed relative to the precursor ion ("*").

While the effect of •NO was very noticeable on the triplet lifetime, it is necessary to expand the y-axis to observe any change on the mass spectrum (Figure 4). Nevertheless, several peaks appear in the presence of •NO and upon irradiation at 488

nm. Figure 4 compares mass spectra after 500 ms irradiation at 488 nm for several reaction times with •NO (and a control without •NO). It shows that $^3Rh6G^+$ reacts with •NO to give peaks at *m/z* 442.2 and *m/z* 472.2, corresponding respectively to $[Rh6G\ -H]^{\bullet+}$ and $[Rh6G\ -H\ +NO]^+$. The trends in intensity variations suggest that these product ions may be formed in the following sequence:

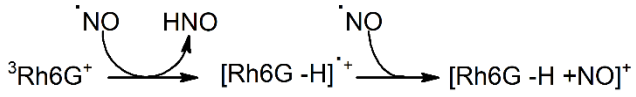


Importantly, no change is observed on the mass spectrum without 488 nm irradiation. These peaks must, therefore, be associated with the specific reactivity of the rhodamine triplet. Remarkably, these specific reaction products are formed continuously during the triplet lifetime (Figures S5, S6 and S7). It is more than 8 orders of magnitude longer than the singlet fluorescence lifetime,[17,18] which rules out any sort of reactivity from the excited singlet state. It is also ~3 orders of magnitude longer than the collisional cooling time determined in the same setup after visible photo-excitation of the chromophore QSY7.[13] Thus, the formation of these reaction products is not likely to be associated with vibrationally hot singlets produced by the CW laser: these hot singlets are indubitably formed, as attested by the appearance of fragments after irradiation at 488 nm, but they are thermalized within milliseconds in the ion trap once the CW laser is stopped. Additionally, the amount of reaction products scales up with the CW laser power (Figure S4), which is thought to increase the relative population of triplets among Rh6G ions. Hence, the reactivity towards •NO seems truly associated with the presence of rhodamine in its triplet electronic state. One possible origin for this specific reactivity may be linked to the "radical character" of the triplet electronic state.

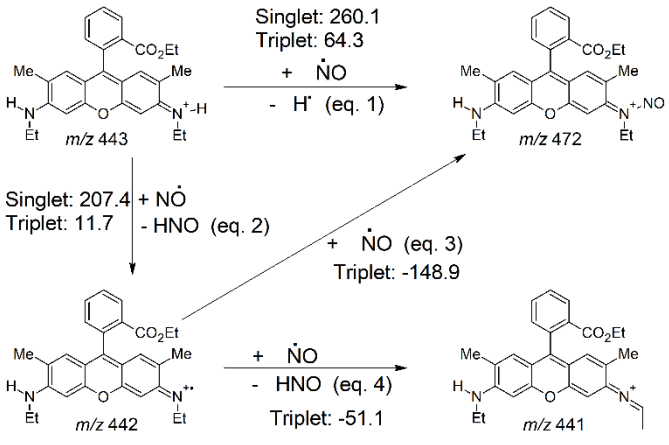


Scheme 2. DFT calculated thermochemistry associated with reaction of triplet with •NO. Singlet/Triplet values refer to reaction enthalpies expressed in $kJ.mol^{-1}$.

Several plausible reaction paths were investigated with DFT computations to determine their respective thermochemistry (see Scheme 2 and the Computations section in ESI for calculation details). The direct mechanism corresponding to the simultaneous H atom loss and addition of •NO is very endothermic, with a reaction enthalpy of 260 $kJ.mol^{-1}$ for the singlet. Even if much less endothermic for the triplet, the reaction enthalpy still amounts to a considerable 64 $kJ.mol^{-1}$ (Scheme 2, eq.1). Alternatively, a two-step mechanism is possible, which firstly involves hydrogen atom abstraction from rhodamine to form $[Rh6G\ -H]^{\bullet+}$ and release nitroxyl (HNO) (Scheme 2, eq.2), followed by the addition of a second •NO yielding nitroso-rhodamine, $[Rh6G\ -H\ +NO]^+$ (Scheme 2, eq.3). Here again, the first step is highly endothermic for the singlet (207 $kJ.mol^{-1}$), which explains that neither the direct nor the two-step mechanism takes place without irradiation at 488 nm. In contrast, the dehydrogenation step is only mildly endothermic (12 $kJ.mol^{-1}$) for the triplet, and should be viable under the experimental conditions of the ion trap. The subsequent •NO addition is highly exothermic (-149 $kJ.mol^{-1}$). Overall, this sequential mechanism seems more likely and would explain the triplet specificity. It is also consistent with the transient observation of the dehydrogenated intermediate at *m/z* 442.2 (Figure 4). A second hydrogen abstraction reaction from $[Rh6G\ -H]^{\bullet+}$ to form $[Rh6G\ -2H]^+$ was also envisaged and calculated to be exothermic (-51 $kJ.mol^{-1}$, Scheme 2, eq. 4). However it is 3 times less favored than the •NO addition and it is not observed experimentally.

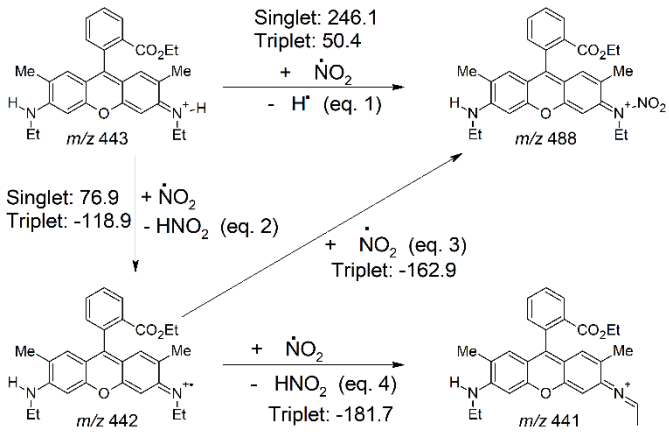


Scheme 3. DFT calculated thermochemistry associated with reaction of triplet with •$NO_2$. Singlet/Triplet values refer to reaction enthalpies expressed in $kJ.mol^{-1}$.

The reactivity of rhodamine triplet towards •$NO_2$ was also examined: during the first hours after the installation of the Helium: •NO line, reaction between •NO and adventitious $O_2$ produces •$NO_2$.[53,54] Even though the presence of radical •$NO_2$ is fortuitous in our experiment, similar reaction mechanisms can be envisaged (Scheme 3). The endothermicity again discounts any possibility of the singlet reacting with •$NO_2$ (direct mechanism: 246 $kJ.mol^{-1}$ and 76 $kJ.mol^{-1}$ *via* first dehydrogenation). However, the hydrogen abstraction from the triplet is highly exothermic (-119 $kJ.mol^{-1}$). Also, in contrast to the reaction with •NO, a second hydrogen abstraction reaction to form $[Rh6G\ -\ 2H]^+$ (-182 $kJ.mol^{-1}$) now competes favorably with the formation of the nitro-rhodamine $[Rh6G\ -H\ +NO_2]^+$ (-163 $kJ.mol^{-1}$). Although this result has to be taken with caution

since it relies on a purely opportunistic measurement, it is consistent with the observation, under these experimental conditions, of a double-dehydrogenation peak at $\Delta m/z$ = -2 (*m/z* 441.2) together with the nitro-rhodamine peak at *m/z* 488.2 in the mass spectrum (Figure 5). Altogether, it also strengthens the interpretation of the results on •NO and the hypothesis that $^3$Rh6G$^+$ cations present a specific reactive character as compared to its ground state singlet counterpart.

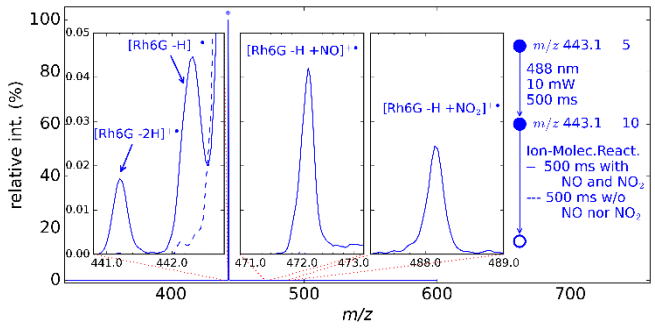


Figure 5. Mass spectrum measured after 500 ms irradiation at 488 nm ($MS^2$) followed by an $MS^3$ step of 500 ms in presence of •NO and •$NO_2$ (—) in the ion trap. The mass spectrum recorded in helium only is presented for comparison (---). Left, center and right inserts focus on the $[Rh6G - H]^{\bullet+}$, $[Rh6G - 2H]^+$, $[Rh6G -H +NO]^+$ and $[Rh6G -H +NO_2]^+$ product ion peaks. In the presence of •NO and •$NO_2$, both singly and doubly dehydrogenated rhodamine peaks are observed at *m/z* 442.2 and *m/z* 441.2 respectively. Both nitroso- and nitro-rhodamine are also observed at *m/z* 472.2 and *m/z* 488.2. Intensities are relative to the precursor ion ("*").

## Competition between reaction and quenching

The effect of collisions between $^3$Rh6G$^+$ and •NO was measured in terms of triplet lifetime shortening. Mass spectrometry observations reveal the existence of a specific chemical reactivity path of deactivation of the triplet. However, the low amount of reaction products detected suggests that non-reactive collisional quenching back to the singlet manifold plays an important role. The competition between the two processes has yet to be characterized. In other words, it would be important from a physical-chemistry point of view to determine how much reactive collisions contribute to the lifetime shortening of the triplet.

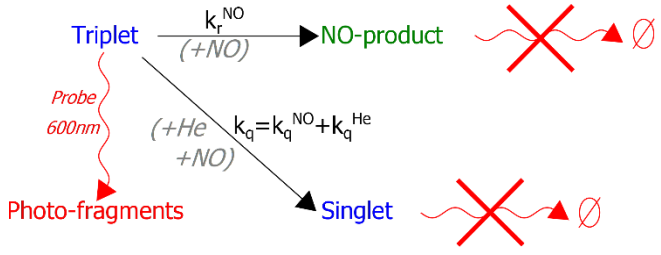


Scheme 4. Schematic representation of the experiment with •NO: $^3$Rh6G$^+$ can react with •NO or be quenched back to the singlet state – by collisions with •NO or simply radiatively (such as in He). Each color represents ions with different *m/z*. Reaction products appear as distinct features on the mass spectrum. However, triplets and singlets are not distinguishable since they are isobaric (same *m/z*). The specific photo-dissociation products from triplets at 600 nm provides a proxy for the population of triplets.

In order to analyze this competition, a simple kinetic model was built, as illustrated in Scheme 4. This model extracts, from experimental data, numerical information regarding the competition between mere quenching *vs.* chemical reaction upon collision between $^3$Rh6G$^+$ and •NO. The kinetic model is based on simple considerations on the origin and evolution of the different species detected by mass spectrometry: triplets can be quenched back to singlets by emission of photons (as occurs in pure helium conditions, $k_q^{He}$) or collisions (as occurs in He: •NO conditions, $k_q^{\bullet NO}$), both phenomena grouped under the $k_{quenching}$ (or $k_q$) rate constant. Triplets can also react with •NO, as was demonstrated above. Although the reaction with •NO was shown to occur *via* a two-step mechanism, extracting the intensity of the intermediate $[Rh6G -H]^{\bullet+}$ ion proved difficult due to the proximity of the Rh6G$^+$ ion peak with intensity ~ 4 orders of magnitude higher. Also, DFT calculations indicate that the second step leading to the [Rh6G -H +NO] product is highly exothermic while the first step is endothermic. Thus, a simple reactive model was adopted where only the first, rate-limiting step is considered in the generation of the nitroso-product, with the $k_{reaction}$ (or $k_r^{\bullet NO}$) rate constant. From this simple model, population equations can be written and, in the steady state approximation for •NO, the system can be integrated and the relative populations of triplets (T) and reaction products (P) can be expressed as a function of time (see Eqs. 1).

$$\begin{cases} T(t) = T_0 . e^{-(k_r^{\bullet NO} + k_q).t} & \text{(1a)} \\ P(t) = \dfrac{k_r^{\bullet NO} . T_0}{k_r^{\bullet NO} + k_q} . \left(1 - e^{-(k_r^{\bullet NO} + k_q).t}\right) & \text{(1b)} \\ F(t) = T_0 . (1 - e^{-\sigma . \Phi}) . e^{-(k_r^{\bullet NO} + k_q).t} & \text{(1c)} \end{cases}$$

Importantly, singlet and triplet rhodamine have the same *m/z* and cannot be distinguished by mass spectrometry alone. In contrast, the chemical reaction products have different *m/z* values and can thus be directly detected by mass spectrometry. Thus, it is important to include in the model the photo-fragments (F) which are exclusively produced by irradiation of the triplet at 600 nm. In Equation 1c, the term $(1 - e^{-\sigma\Phi})$ is a function of the triplet photo-fragmentation cross section σ and of the probe laser fluence (Φ), the latter being constant for given experimental conditions. Thus, fitting the experimental data with such mono-exponential functions enables the estimation of the triplet lifetimes $1/(k_r^{\bullet NO} + k_q)$ in He:NO (and $1/k_q^{He}$ in helium) (see Supporting Information for details).

The determination of branching ratios between relaxation paths represents an important objective in order to finely understand the physical-chemistry of molecular systems. Here, the branching ratio between •NO reaction and •NO quenching of the triplet: $BR = k_r^{\bullet NO}/(k_r^{\bullet NO} + k_q^{\bullet NO})$, can be extracted from the experimental datasets. In our simple model, this ratio appears hidden in the prefactor of the products population P while using the rate difference in helium and He:NO to estimate $k_r^{NO} + k_q^{NO}$ (see Eq.1b and Eqs.S1). The prefactor on the photo-fragments (F) provides a lowerbound value for the initial triplet population $T_0$ (see Eqs. 1c and S2) from which it is possible to calculate an upper-bound estimate for the reactive branching ratio (see Supporting Information for full details).

Optimized variables are listed in Table 1 together with the upper bound estimation of the reaction/quenching branching ratio. The resulting upper-boundary for the branching ratio is typically lower than 2 %. It means that less than 2 % of collisions with •NO that interact destructively with $^3$Rh6G$^+$ are reactive, the others simply quench it back to the singlet manifold. As expected from the low intensity of product ions on the mass spectra, the majority of collisions between $^3$Rh6G$^+$ and •NO do not lead to chemical modifications.

Table 1. Results of the fits for the fragmentation ratio together with the products ratio, with the total rate constant ($\boldsymbol{k_r^{\bullet NO} + k_q}$) as shared parameter between all datasets.

| | | Exponential fit on Fragments (F) and Products (P) | | |
|---|---|---|---|---|
| | | $\overbrace{\frac{k_r^{\bullet NO}.T_0}{k_r^{\bullet NO}+k_q}}^{fit\ on\ P^a}$ | $\overbrace{T_0.\left(1-e^{-\sigma.\Phi}\right)}^{fit\ on\ F^a}$ | upper bound[b] for $k_r^{\bullet NO}\Big/k_r^{\bullet NO}+k_q^{\bullet NO}$ |
| He:NO | 5 | 1.7 $10^{-4}$ | 8.0 $10^{-2}$ | 0.3 % |
| | 6 | 2.0 $10^{-4}$ | 2.1 $10^{-2}$ | 1.5 % |
| | 7 | 2.0 $10^{-4}$ | 1.9 $10^{-2}$ | 1.7 % |

[a] Prefactors are unit-less. Ion intensities are normalized by the total ion current (TIC) *per* mass spectrum, so that $T_0$ represents the initial *relative* population of triplets. The latter may vary considerably depending on day-to-day experimental conditions (laser alignment, ion signal, *etc.*). As a result, large variations may be observed on absolute intensities. Thus, prefactors are optimized separately *per* dataset. [b] Rate constants $k_q^{He}$ and ($k_r^{\bullet NO}$+$k_q$), which are required to calculate the upper bound (see Eq. S2), were taken from global fits on F: respectively 0.53 $s^{-1}$ and 1.43 $s^{-1}$.

## Conclusions and Perspectives

In conclusion, we have developed a pump-probe approach to study the gas-phase optical spectrum, lifetime and bimolecular reactivity of long-lived $^3$Rh6G$^+$. In pure helium at room temperature (≥ 298 K), the lifetime of $^3$Rh6G$^+$ is close to 1.9 s, which is presumably close to the radiative lifetime. In the presence of •NO, it was shown that the triplet lifetime dropped due both to collisional quenching and reactivity. Globally, it could be estimated that 1 to 15 % of collisions with •NO efficiently deplete the triplets (*i.e.* the majority of collisions with •NO are neither reactive nor inducing triplet quenching).

Among the "efficient" collisions with •NO, less than 2 % are reactive and yield, in a two-step mechanism, the nitroso-rhodamine product. Thus ≥ 98 % of these "efficient" collisions merely quench the triplet back to a singlet state. Interestingly, although the reactive cross section of triplets with •NO is very low compared to triplet deactivation, this type of reaction with free radicals may correspond to a major photo-degradation pathway, particularly in biological media. Cycling through the S1 ← S0 transition for long periods of time, *e.g.* in imaging applications, may amplify the effective yield of this bleaching mechanism. The free radical scavenging character of rhodamine triplets may also induce unwanted alteration of the biological medium during in-vivo imaging. It is, thus, important to take it into account and understand it in order to find ways to minimize or circumvent it. Also, this reactivity occurs during the whole lifetime of rhodamine triplets. The delayed reactivity of photo-excited triplets enables the diffusion of reagents and may result in bimolecular processes difficult to achieve from the excited singlet manifold due much shorter lifetimes.

The optical pump-probe gas-phase approach proposed herein should be generally applicable to other long-lived triplet ions provided that an excitation wavelength unique to the triplet can be found to allow monitoring of the triplet population. Other charged dyes such as Rh575$^+$, RhB$^+$ and Rh101$^+$ that are readily transferred to the gas phase *via* electrospray ionization (ESI) are obvious candidates to extend this study.[15] Using the same setup, it would be possible to explore the reactivity of the rhodamine triplet with various other reagents such as CO or triethylamine (TEA). More generally, it would be interesting to assess the Lewis acidity/basicity of rhodamine triplets by such ion-molecule reactions. The ability to mass select ions derived from dyes should also allow the role of clustering (dimerization, *etc.*) on the triplet lifetime and chemistry to be assessed.

Finally, our approach, which groups under one unique experimental setup the photo-preparation of intermediates, their optical characterization and the ability to monitor reaction products under controlled conditions, paves the way to photo-catalysis studies.

## Author Contributions

The manuscript was written through contributions of all authors. All authors have given approval to the final version of the manuscript.

## Conflicts of interest

There are no conflicts to declare.

## Acknowledgements

This research has received funding from the European Research Council under the European Union's Seventh Framework Program (FP7/2007-2013 Grant agreement N°320659). R.A.J.O thanks the Humboldt foundation for a senior fellowship which facilitated travel to Prof. Manfred Kappes' laboratory for discussions and the University of Melbourne for short study leave. The authors thank Profs. Evan Bieske, Ken Ghiggino and Dr. Wallace Wong for useful discussions.

## Notes and references

§ The NCE concept is specific to Thermo Fisher Scientific ion traps and accounts for the near linear correlation between the collision energy required to achieve optimum fragmentation efficiency of an ion with its $m/z$ value, see ref[47] for details.

1 M. Beija, C. A. M. Afonso and J. M. G. Martinho, Synthesis and applications of Rhodamine derivatives as fluorescent probes, *Chem. Soc. Rev.*, 2009, **38**, 2410.

2 A. S. Klymchenko, Solvatochromic and Fluorogenic Dyes as Environment-Sensitive Probes: Design and Biological Applications, *Acc. Chem. Res.*, 2017, **50**, 366–375.

3 K. Kaur, R. Saini, A. Kumar, V. Luxami, N. Kaur, P. Singh and S. Kumar, Chemodosimeters: An approach for detection and estimation of biologically and medically relevant metal ions, anions and thiols, *Coord. Chem. Rev.*, 2012, **256**, 1992–2028.

4 J. Chan, S. C. Dodani and C. J. Chang, Reaction-based small-molecule fluorescent probes for chemoselective bioimaging, *Nat. Chem.*, 2012, **4**, 973–984.

5 L. Yuan, W. Lin, K. Zheng and S. Zhu, FRET-Based Small-Molecule Fluorescent Probes: Rational Design and Bioimaging Applications, *Acc. Chem. Res.*, 2013, **46**, 1462–1473.

6 I. Ghosh, L. Marzo, A. Das, R. Shaikh and B. König, Visible Light Mediated Photoredox Catalytic Arylation Reactions, *Acc. Chem. Res.*, 2016, **49**, 1566–1577.

7 S. Becker, I. Gregor and E. Thiel, Photoreactions of rhodamine dyes in basic solvents, *Chem. Phys. Lett.*, 1998, **283**, 350–356.

8 M. Heupel, I. Gregor, S. Becker and E. Thiel, Photophysical and photochemical properties of electronically excited fluorescent dyes: a new type of time-resolved laser-scanning spectroscopy, *Int. J. Photoenergy*, 1999, **1**, 165–172.

9 S. Daly, F. Poussigue, A.-L. Simon, L. MacAleese, F. Bertorelle, F. Chirot, R. Antoine and P. Dugourd, Action-FRET: Probing the Molecular Conformation of Mass-Selected Gas-Phase Peptides with Förster Resonance Energy Transfer Detected by Acceptor-Specific Fragmentation, *Anal. Chem.*, 2014, **86**, 8798–8804.

10 S. Daly, C. M. Choi, F. Chirot, L. MacAleese, R. Antoine and P. Dugourd, Action-Self Quenching: Dimer-Induced Fluorescence Quenching of Chromophores as a Probe for Biomolecular Structure, *Anal. Chem.*, 2017, **89**, 4604–4610.

11 S. Daly, A. J. Kulesza, G. Knight, L. MacAleese, R. Antoine and P. Dugourd, Visible and Ultraviolet Spectroscopy of Gas Phase Rhodamine 575 Cations, *J. Phys. Chem. A*, 2015, **119**, 5634–5641.

12 A. J. Kulesza, E. Titov, S. Daly, R. Włodarczyk, J. Megow, P. Saalfrank, C. M. Choi, L. MacAleese, R. Antoine and P. Dugourd, Excited States of Xanthene Analogues: Photofragmentation and Calculations by CC2 and Time-Dependent Density Functional Theory, *ChemPhysChem*, 2016, **17**, 3129–3138.

13 M. Bouakil, A. J. Kulesza, S. Daly, L. MacAleese, R. Antoine and P. Dugourd, Visible Multiphoton Dissociation of Chromophore-Tagged Peptides, *J. Am. Soc. Mass Spectrom.*, 2017, **28**, 2181–2188.

14 M. Kordel, D. Schooss, C. Neiss, L. Walter and M. M. Kappes, Laser-induced fluorescence of rhodamine 6G cations in the gas phase: A lower bound to the lifetime of the first triplet state, *J. Phys. Chem. A*, 2010, **114**, 5509–5514.

15 J. F. Greisch, M. E. Harding, M. Kordel, W. Klopper, M. M. Kappes and D. Schooss, Intrinsic fluorescence properties of rhodamine cations in gas-phase: Triplet lifetimes and dispersed fluorescence spectra, *Phys. Chem. Chem. Phys.*, 2013, **15**, 8162–8170.

16 I. Carmichael and G. L. Hug, Triplet–Triplet Absorption Spectra of Organic Molecules in Condensed Phases, *J. Phys. Chem. Ref. Data*, 1986, **15**, 1–250.

17 M. Savarese, A. Aliberti, I. De Santo, E. Battista, F. Causa, P. A. Netti and N. Rega, Fluorescence Lifetimes and Quantum Yields of Rhodamine Derivatives: New Insights from Theory and Experiment, *J. Phys. Chem. A*, 2012, **116**, 7491–7497.

18 A. M. Nagy, F. O. Talbot, M. F. Czar and R. A. Jockusch, Fluorescence lifetimes of rhodamine dyes in vacuo, *J. Photochem. Photobiol. A Chem.*, 2012, **244**, 47–53.

19 M. J. McEwan and L. Phillips, Chemistry in the upper atmosphere, *Acc. Chem. Res.*, 1970, **3**, 9–17.

20 M. T. Bowers, P. R. Kemper and J. B. Laudenslager, Reactions of ions in excited electronic states: $(N_2^{+\cdot})^* + N_2 \rightarrow N_3^+ + N$, *J. Chem. Phys.*, 1974, **61**, 4394–4399.

21 O. Asvany, Understanding the Infrared Spectrum of Bare CH5+, *Science (80-. ).*, 2005, **309**, 1219–1222.

22 S. Zhou, M. Schlangen and H. Schwarz, Spin-Selective, Competitive Hydrogen-Atom Transfer versus CH 2 O-Generation from the CH 4 /[ReO 4 ] + Couple at Ambient Conditions, *Chem. - A Eur. J.*, 2017, **23**, 17469–17472.

23 C.-Y. Ng, Y. Xu, Y.-C. Chang, A. Wannenmacher, M. Parziale and P. B. Armentrout, Quantum electronic control on chemical activation of methane by collision with spin–orbit state selected vanadium cation, *Phys. Chem. Chem. Phys.*, 2021, **23**, 273–286.

24 M. Tichý, A. B. Rakshit, D. G. Lister, N. D. Twiddy, N. G. Adams and D. Smith, A study of the reactions of the ground and metastable states of C+, N+, S+ and N2+ at 300 K, *Int. J. Mass Spectrom. Ion Phys.*, 1979, **29**, 231–247.

25 B. H. Mahan, C. Martner and A. O'Keefe, Laser induced fluorescence studies of the charge transfer reactions of N 2 + with Ar and N 2, *J. Chem. Phys.*, 1982, **76**, 4433–4438.

26 D. H. Russell, J. V. B. Oriedo and T. Solouki, in *Organometallic Ion Chemistry*, ed. B. S. Freiser, Springer, 1996, pp. 197–228.

27 M. T. Bowers, P. R. Kemper, G. von Helden and P. A. M. van Koppen, Gas-Phase Ion Chromatography: Transition Metal State Selection and Carbon Cluster Formation, *Science (80-. ).*, 1993, **260**, 1446–1451.

28 S. Kato, M. J. Frost, V. M. Bierbaum and S. R. Leone, A selected ion flow tube-laser induced fluorescence instrument for vibrationally state-specific ion-molecule reactions, *Rev. Sci. Instrum.*, 1993, **64**, 2808–2820.

29 S. L. Anderson, Mode-Selective Differential Scattering as a Probe of Polyatomic Ion Reaction Mechanisms, *Acc. Chem. Res.*, 1997, **30**, 28–36.

30 R. N. Zare, Laser Control of Chemical Reactions, *Science (80-. ).*, 1998, **279**, 1875–1879.

31 S. Schlemmer, E. Lescop, J. von Richthofen, D. Gerlich and M. A. Smith, Laser induced reactions in a 22-pole ion trap: C2H2++hv3+H2→C2H3++H, *J. Chem. Phys.*, 2002, **117**, 2068–2075.

32 A. J. Göttle, F. Alary, I. M. Dixon, J.-L. Heully and M. Boggio-Pasqua, Unravelling the S → O Linkage Photoisomerization Mechanisms in cis - and trans -[Ru(bpy) 2 (DMSO) 2 ] 2+ Using Density Functional Theory, *Inorg. Chem.*, 2014, **53**,


 

6752–6760.

33 C. M. Choi, L. MacAleese, P. Dugourd, M. C. Choi and F. Chirot, Photo-induced linkage isomerization in the gas phase probed by tandem ion mobility and laser spectroscopy, *Phys. Chem. Chem. Phys.*, 2018, **20**, 12223–12228.

34 M. S. Scholz, J. N. Bull, E. Carrascosa, B. D. Adamson, G. K. Kosgei, J. J. Rack and E. J. Bieske, Linkage Photoisomerization of an Isolated Ruthenium Sulfoxide Complex: Sequential versus Concerted Rearrangement, *Inorg. Chem.*, 2018, **57**, 5701–5706.

35 M. Polášek, F. Tureček, P. Gerbaux and R. Flammang, Nitrobenzene Isomers, *J. Phys. Chem. A*, 2001, **105**, 995–1010.

36 W. C. Lineberger and W. T. Borden, The synergy between qualitative theory, quantitative calculations, and direct experiments in understanding, calculating, and measuring the energy differences between the lowest singlet and triplet states of organic diradicals, *Phys. Chem. Chem. Phys.*, 2011, **13**, 11792.

37 T. Tidwell, Sunlight and free radicals, *Nat. Chem.*, 2013, **5**, 637–639.

38 A. Downes and T. P. Blunt, The effect of sunlight upon hydrogen peroxide., *Nature,* 1879, **20**, 521–521.

39 L. MacAleese, S. Hermelin, K. El Hage, P. Chouzenoux, A. J. Kulesza, R. Antoine, L. Bonacina, M. Meuwly, J.-P. Wolf and P. Dugourd, Sequential Proton Coupled Electron Transfer (PCET): Dynamics Observed over 8 Orders of Magnitude in Time, *J. Am. Chem. Soc.*, 2016, **138**, 4401–4407.

40 M. J. Frisch, G. W. Trucks, H. B. Schlegel, G. E. Scuseria, M. A. Robb, J. R. Cheeseman, G. Scalmani, V. Barone, G. A. Petersson, H. Nakatsuji, X. Li, M. Caricato, A. V. Marenich, J. Bloino, B. G. Janesko, R. Gomperts, B. Mennucci, H. P. Hratchian, J. V. Ortiz, A. F. Izmaylov, J. L. Sonnenberg, D. Williams-Young, F. Ding, F. Lipparini, F. Egidi, J. Goings, B. Peng, A. Petrone, T. Henderson, D. Ranasinghe, V. G. Zakrzewski, J. Gao, N. Rega, G. Zheng, W. Liang, M. Hada, M. Ehara, K. Toyota, R. Fukuda, J. Hasegawa, M. Ishida, T. Nakajima, Y. Honda, O. Kitao, H. Nakai, T. Vreven, K. Throssell, J. A. J. Montgomery, J. E. Peralta, F. Ogliaro, M. J. Bearpark, J. J. Heyd, E. N. Brothers, K. N. Kudin, V. N. Staroverov, T. A. Keith, R. Kobayashi, J. Normand, K. Raghavachari, A. P. Rendell, J. C. Burant, S. S. Iyengar, J. Tomasi, M. Cossi, J. M. Millam, M. Klene, C. Adamo, R. Cammi, J. W. Ochterski, R. L. Martin, K. Morokuma, O. Farkas, J. B. Foresman and D. J. Fox, 2016.

41 A. M. Brouwer, Standards for photoluminescence quantum yield measurements in solution (IUPAC Technical Report), *Pure Appl. Chem.*, 2011, **83**, 2213–2228.

42 W. A. Donald, R. D. Leib, M. Demireva, B. Negru, D. M. Neumark and E. R. Williams, "Weighing" Photon Energies with Mass Spectrometry: Effects of Water on Ion Fluorescence, *J. Am. Chem. Soc.*, 2010, **132**, 6904–6905.

43 A. K. Chibisov and T. D. Slavnova, The study of the photophysics and primary photochemistry of rhodamine 6G aggregates, *J. Photochem.*, 1978, **8**, 285–297.

44 A. Dunne and M. F. Quinn, Triplet–triplet absorption spectra and the spectra of the photoreduced states of Rhodamine B and Rhodamine 110, *J. Chem. Soc. Faraday Trans. 1 Phys. Chem. Condens. Phases*, 1977, **73**, 1104.

45 B. R. V. Ferreira, D. N. Correa, M. N. Eberlin and P. H. Vendramini, Fragmentation Reactions of Rhodamine B and 6G as Revealed by High Accuracy Orbitrap Tandem Mass Spectrometry, *J. Braz. Chem. Soc.*, 2017, **28**, 136–142.

46 J. Peters, M. Clemen and J. Grotemeyer, Fragmentation of deuterated rhodamine B derivates by laser and collisional activation in an FT-ICR mass spectrometer, *Anal. Bioanal. Chem.*, 2013, **405**, 7061–7069.

47 L. L. Lopez, P. R. Tiller, M. W. Senko and J. C. Schwartz, Automated strategies for obtaining standardized collisionally induced dissociation spectra on a benchtop ion trap mass spectrometer, *Rapid Commun. Mass Spectrom.*, 1999, **13**, 663–668.

48 R. G. Cooks, D. Zhang, K. J. Koch, F. C. Gozzo and M. N. Eberlin, Chiroselective Self-Directed Octamerization of Serine: Implications for Homochirogenesis, *Anal. Chem.*, 2001, **73**, 3646–3655.

49 C. K. Barlow, A. Wright, C. J. Easton and R. A. J. O'Hair, Gas-phase ion-molecule reactions using regioselectively generated radical cations to model oxidative damage and probe radical sites in peptides, *Org. Biomol. Chem.*, 2011, **9**, 3733.

50 K. F. Lim, *COLRATE. QCPE 643: Calculation of gas-kinetic collision rate coefficients, Quantum Chem. Progr. Exch. Bull., 1994, 14 (1). The program Colrate is available for download from the author 's website at Deakin University, Geelong,Victoria, Australia: http://www.deakin.edu.au/~lim/programs/COLRATE.html.*

51 T. Su and M. T. Bowers, Ion-Polar molecule collisions: the effect of ion size on ion-polar molecule rate constants; the parameterization of the average-dipole-orientation theory, *Int. J. Mass Spectrom. Ion Phys.*, 1973, **12**, 347–356.

52 T. P. Second, J. D. Blethrow, J. C. Schwartz, G. E. Merrihew, M. J. MacCoss, D. L. Swaney, J. D. Russell, J. J. Coon and V. Zabrouskov, Dual-pressure linear ion trap mass spectrometer improving the analysis of complex protein mixtures, *Anal. Chem.*, 2009, **81**, 7757–7765.

53 P. G. Ashmore, M. G. Burnett and B. J. Tyler, Reaction of nitric oxide and oxygen, *Trans. Faraday Soc.*, 1962, **58**, 685.

54 O. B. Gadzhiev, S. K. Ignatov, S. Gangopadhyay, A. E. Masunov and A. I. Petrov, Mechanism of Nitric Oxide Oxidation Reaction (2NO + O 2 → 2NO 2 ) Revisited, *J. Chem. Theory Comput.*, 2011, **7**, 2021–2024.